Graefe's Archive for Clinical and Experimental Ophthalmology (2020) 258:2059–2068
https://doi.org/10.1007/s00417-020-04633-8

PEDIATRICS

Effects of iron deficiency anemia on peripapillary and macular vessel density determined using optical coherence tomography angiography on children

Muhammet Furkan Korkmaz[1] · Mehmet Erol Can[2] · Elif Güler Kazancı[3]

Received: 19 September 2019 / Revised: 12 February 2020 / Accepted: 17 February 2020 / Published online: 3 March 2020

Abstract

Purpose To evaluate retinal vascular parameters by optical coherence tomography angiography (OCT-A) in iron deficiency anemia (IDA).

Methods Thirty-two patients with IDA (study group) and 30 healthy children (control group) were enrolled in the study. All subjects underwent a complete ocular examination. OCT-A scans were performed in a 6 × 6 mm area centered on the macula. Foveal avascular zone (FAZ), non-flow area (NFA), FAZ perimeter (PERIM), acircularity index (AI) of FAZ, and foveal density (FD) were measured in the superficial capillary plexus (SCP) and deep capillary plexus (DCP). SCP and DCP were also scanned centered on the optic disk. Hemoglobin (Hb), mean corpuscular volume (MCV), serum iron, total iron-binding capacity (TIBC), and ferritin were also studied and compared for both groups.

Results The mean age was 12.22 ± 4.48 years (ranged 5–18 years) in the study group and 12.37 ± 3.76 years (ranged 6–18 years) in the control group. The mean FAZ value was 0.290 ± 0.09 mm^2 in the study group and 0.298 ± 0.11 mm^2 in the control group. The mean NFA value was 0.477 ± 0.10 mm^2 in the study group and 0.486 ± 0.13 mm^2 in the control group ($p > 0.05$). FD and AI were not statistically significant between the study group and control group ($p > 0.05$). The mean value for SCP was statistically significant between the study group and control group ($p < 0.05$). The mean value for DCP was not significantly different between the study and control groups ($p > 0.05$). The mean values for capillary density on optic disk were also statistically significant between the study group and control group ($p < 0.05$). A negative correlation was found between serum iron, TIBC, and capillary plexus density ($p < 0.05$). A positive correlation was found between MCV and ferritin values and capillary plexus density ($p < 0.05$).

Conclusion IDA had significantly lower capillary plexus density. We detected retinal microvascular changes in young IDA patients before significant ocular anomalies, especially ischemic changes, developed.

Keywords Iron deficiency anemia · Optical coherence tomography angiography · Foveal density · Deep capillary plexus · Superficial capillary plexus · Peripapillary retinal capillary density

Introduction

Iron deficiency anemia (IDA) is still the most common etiology of nutritional anemia in the pediatric age group worldwide [1]. The etiology of iron deficiency (ID) includes dietary deficiency, blood loss, and metabolic causes [2]. Iron is very important for oxygen transport; besides, it has an important role associated with the central nervous system including normal myelinization, neurotransmitter synthesis, and neurometabolism [3]. ID causes developmental abnormalities, ischemic stroke, venous thrombosis, breath-holding episodes, and other neurologic problems in children [4]. The exact

✉ Muhammet Furkan Korkmaz
korkmazmfurkan@gmail.com

[1] Department of Pediatrics, Yuksek Ihtisas Training and Research Hospital, University of Health Sciences, Bursa, Turkey

[2] Department of Ophthalmology, Bursa City Hospital, Bursa, Turkey

[3] Department of Pediatric Hematology, Yuksek Ihtisas Training and Research Hospital, University of Health Sciences, Bursa, Turkey

pathophysiology of fundus lesions is still unknown, but it is considered that it might be associated with hypoxia [5, 6].

Optical coherence tomography angiography (OCT-A) is a new imaging method that can be used non-invasively without the need of an intravenous contrast agent. The sequential optical coherence tomography scans provide a detailed image of the retinal vascular network by obtaining and processing the motion contrast of erythrocytes in the vessels in the specific retina area [7]. OCT-A displays the blood flow in various layers of the retina in high resolution and rapidly provides three-dimensional images of these vascular layers. This feature allows quantitative measurement of neovascular formation areas and blood flow in these vessels [8]. Recently, OCT-A is used to identify vascular abnormalities associated with sickle cell disease, retinopathy of prematurity, and diabetic retinopathy in the pediatric age group [9–11]. With known advantages, OCT-A may provide an exciting opportunity to advance the understanding of vascular changes occurring in ocular tissues in IDA. In the present study, we aimed to investigate retinal microvascular changes in children with IDA by using OCT-A.

Methods

Study population and design

This study was carried out as a single-center and prospective cross-sectional study among 32 patients with IDA and 30

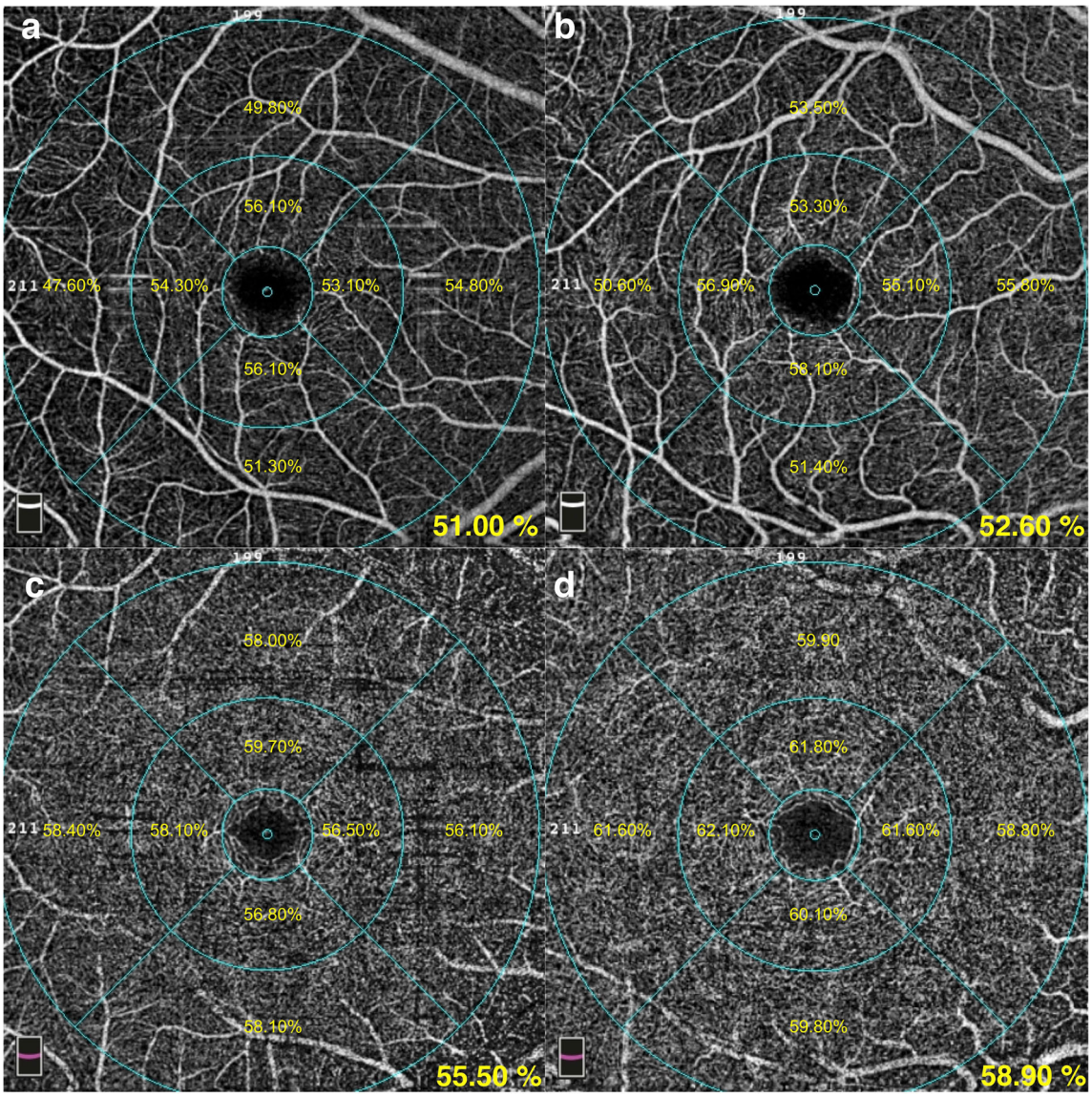

Fig. 1 Impression of foveal centered capillary plexus density in IDA and healthy control. **a** Vessel density (VD) in the superficial capillary plexus with iron deficiency anemia (IDA). **b** In healthy control. **c** VD in the deep capillary plexus with IDA. **d** In healthy control

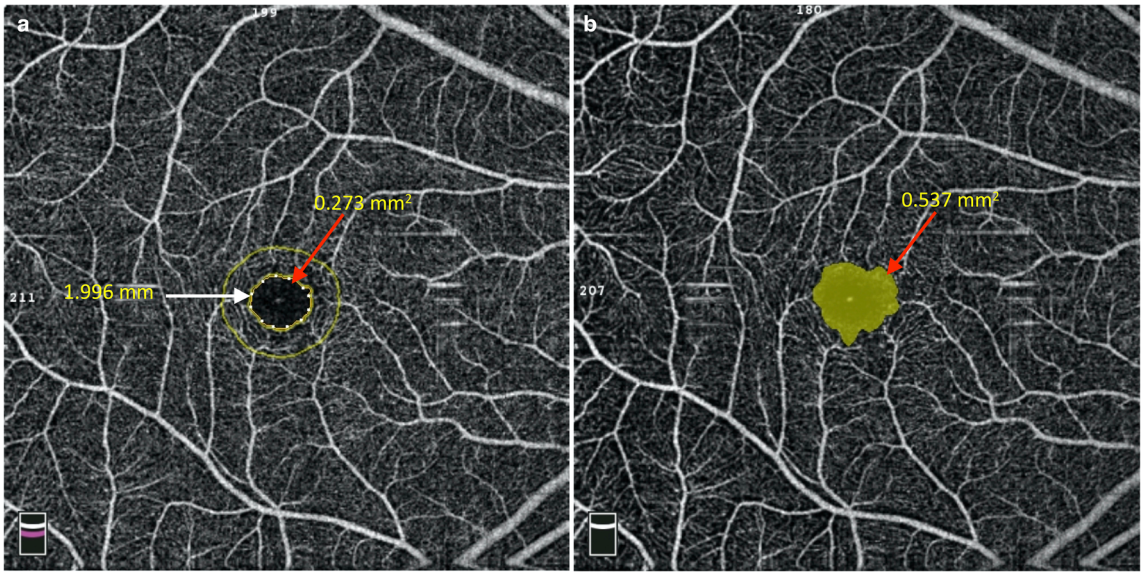

Fig. 2 **a** Foveal avascular zone (FAZ) indicated by the red arrow and FAZ perimeter indicated by the white arrow. **b** Non-flow area (indicated by the red arrow) in the superficial capillary plexus

healthy children. The study was conducted between January 2019 and June 2019 in the Department of Pediatric Hematology and the Department of Ophthalmology of the University of Health Sciences Yuksek Ihtisas Training and Research Hospital, Bursa, Turkey (a tertiary care hospital with a total of 1600 beds including 200 for pediatric patients). The study was approved by the local ethics committee (2011-KAEK-252018/12-24). Before inclusion in the study, written

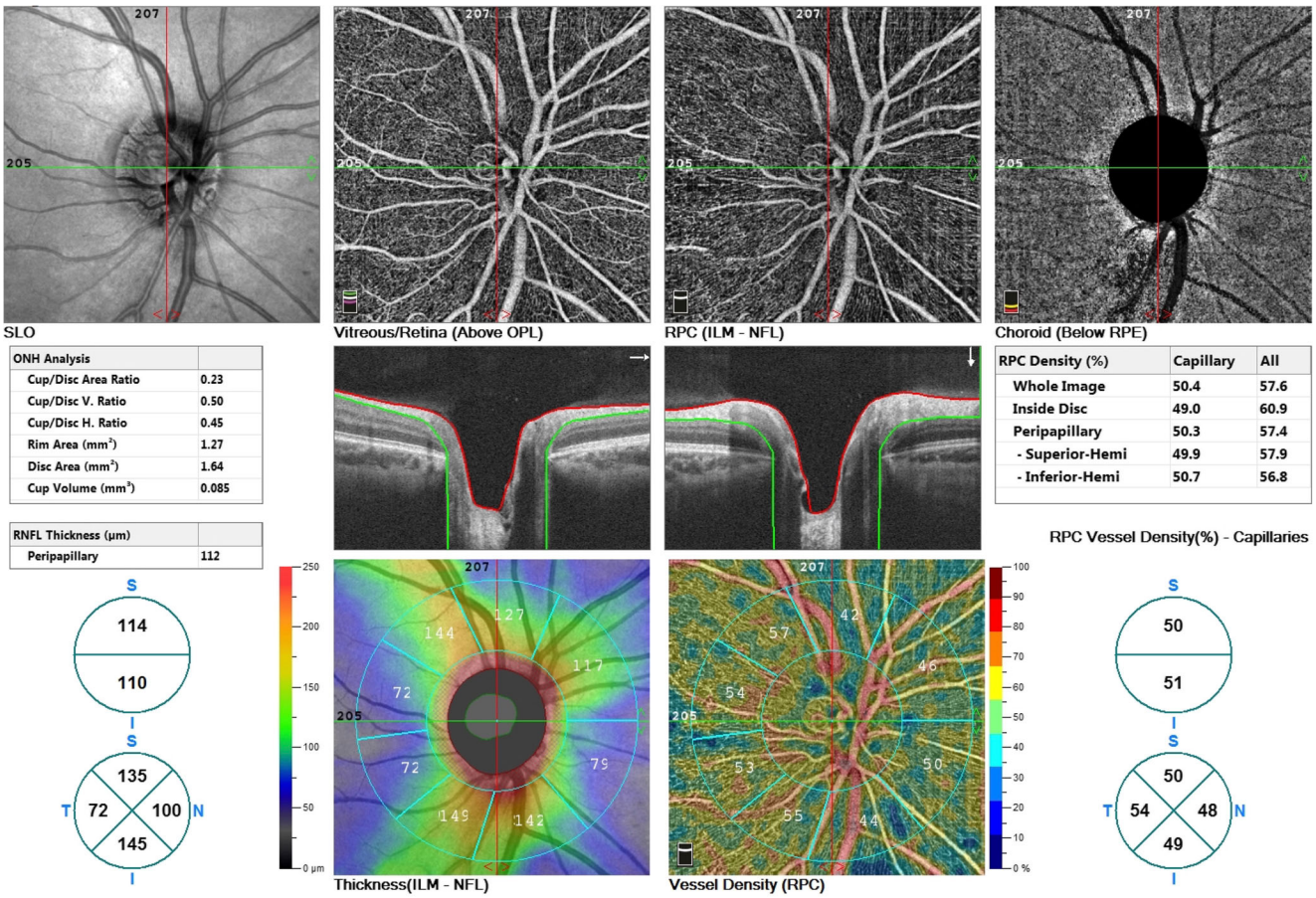

Fig. 3 Impression of optic disk centered capillary plexus density in different quadrants

Table 1 Demographics and clinical characteristics of participants

Parameters	Study group ($n = 32$)	Control group ($n = 30$)	p value
Age (years)*	12.22 ± 4.48	12.37 ± 3.76	0.843[a]
Female/male	20/12	16/14	0.363[b]
Hemoglobin (g/dL)*	10.31 ± 1.47	12.78 ± 0.64	< 0.001[a]
MCV (μg/dL)*	71.62 ± 8.86	81.93 ± 3.37	< 0.001[a]
Serum iron (μg/dL)*	41.70 ± 29.54	84.25 ± 19.42	< 0.001[a]
TIBC*	376.24 ± 96.42	295.92 ± 62.18	< 0.001[a]
Ferritin (nmole/L)*	29.52 ± 47.43	67.25 ± 22.68	< 0.001[a]

Abbreviations: *MCV*, mean corpuscular volume; *TIBC*, total iron-binding capacity

*The values are presented as mean ± standard deviation

[a] Independent samples *t* test

[b] Chi-square test

informed consent was obtained from all parents or legal tutors of the patients.

Examination protocol and study measurements

The IDA group consisted of children with a hemoglobin (Hb) level of < 11.5 g/dL, a mean corpuscular volume (MCV) of < 77 fL, and serum ferritin of < 12 ng/mL. The control group consisted of healthy volunteers under the care of general pediatrics counseling for a routine eye examination and who had Hb levels of > 12 g/dL and ferritin levels of > 12 ng/mL.

All participants underwent a complete ophthalmologic examination including best-corrected visual acuity, slit lamp biomicroscopy, Goldmann applanation tonometry, perimetry, and fundus examination.

OCT-A measurement

Refractive error measurements were performed with the same automatic refractor-keratometer device. XR Avanti Optical Coherence Tomography Angiography with AngioVue (RTVue XR AVANTI, Optovue, Fremont, CA, USA) was used to measure 6 mm × 6 mm macular images centered on the foveola. Also, 4.5 × 4.5 mm optic disk images of each patient were obtained. All OCT-A measurements were made by the same doctor (M.E.C.) and made between the same hour interval (09:00–12:00). Three consecutive measurements were made in each eye of each patient, and the best image quality measurements were used to obtain data (quality score > 7). This method is based on detailed imaging of the retinal vessel network by obtaining and processing the motion contrast of erythrocytes in the vessels through sequential OCT scans of a specific retinal area. Using the software in the OCT-A (the software in our device, AngioVue), in the 6 × 6 mm measuring mode, on the foveal, centered on three main areas: capillary plexus density can be detected in the foveal, parafoveal, and perifoveal quadrants. The innermost ring refers to a foveal region of 1 mm, the middle ring refers to a parafoveal region of 3 mm, and the distal ring of a 6-mm perifoveal region. Besides, these zones are separated with a software to four main equal quadrants (nasal, temporal, superior, and inferior) and to 2 equal hemispheres (superior and inferior) (Fig. 1). AngioVue software can visualize the vascular network of the retina and choroid layer-by-layer and provides three-dimensional images of these vascular layers. The superficial capillary plexus (SCP) was

Table 2 Comparison of the non-flow and foveal avascular zone assessment tool parameters in both groups

	Study group ($n = 33$)	Control group ($n = 29$)	p[a] value
Non-flow area (mm^2) (SCP)	0.477 ± 0.10	0.486 ± 0.13	0.694
FAZ area (mm^2) (whole retina)	0.290 ± 0.09	0.298 ± 0.11	0.688
FAZ perimeter (mm)	2.04 ± 0.37	2.06 ± 0.43	0.826
AI	1.09 ± 0.02	1.08 ± 0.02	0.656
FD (%)	56.85 ± 3.48	57.62 ± 3.66	0.251

Abbreviations: *SCP*, superficial capillary plexus; *FAZ*, foveal avascular zone; *AI*, acircularity index; *FD*, foveal density

[a] Independent samples *t* test

automatically segmented between the internal limiting membrane (ILM) to the outer boundary of the inner plexiform layer (IPL). The deep capillary plexus (DCP) was automatically segmented between an inner boundary of the IPL and outer boundary of the IPL. The vessel density (VD) shows the percentage (%) area occupied by microvasculature in the segmented area. The peripapillary region was defined as a 4.5 × 4.5 mm wide annulus centered on the optic disk (OD). The VD within this region was measured from the ILM to the posterior boundary of the retinal nerve fiber layer (RNFL). The foveal vascular zone (FAZ) area was measured using a slab from the ILM to the retinal pigment epithelium (RPE). Non-flow area (NFA) in the SCP and FAZ area in the whole retina were automatically obtained by the software. FAZ perimeter (PERIM) and acircularity index (AI) were also automatically obtained from the whole retina. Foveal density (FD) is the vessel density 300 mm around the FAZ and is evaluated as FAZ parameters (Fig. 2). Also, 4.5 × 4.5 mm optic disk scans of each patient were measured (Fig. 3).

Exclusion criteria

Ocular exclusion criteria for this study are as follows: prior history of significant ocular disease, a best-corrected visual acuity worse than 20/20, amblyopia, more than 2 diopters of cylindrical and/or 4 diopters of spherical refractive error, intraocular pressure readings greater than 21 mmHg, the use of topical medication, active corneal lesion, glaucoma, history of uveitis, retinal disease, ocular trauma or tumor, poor image quality, dense media opacities. Extraocular exclusion criteria for this study are associated systemic disorders that might affect the eyes (e.g., uncontrolled diabetes or hypertension). Finally, the patients who did not agree to be examined using the required OCT-A were excluded.

Statistical analysis

All statistical analyses were performed using SPSS (Statistical Package for the Social Sciences) version 21. Measurements taken from both eyes per subject were selected for the analyses. For each continuous variable, data normality was confirmed using the Kolmogorov–Smirnov test ($p > 0.05$). Pearson's correlation was used to examine the relationships among the measured variables. For the comparison of the study group and the control group, an independent sample t test was performed for normally distributed data. In comparison of categorical variables, chi-square test was utilized. p values less than 0.05 were considered significant.

Table 3 Deep capillary plexus and superficial capillary plexus densities in the different quadrants in the foveal, perifoveal, and parafoveal areas

	Study group*	Control group*	p[a] value
Vessel density, SCP flow (%)			
Whole retina	50.42 ± 2.49	51.72 ± 1.92	0.002
Superior-hemi	50.41 ± 2.60	51.77 ± 1.98	0.002
Inferior-hemi	50.42 ± 2.52	51.65 ± 2.09	0.005
Fovea	22.26 ± 6.18	21.53 ± 6.50	0.534
Parafovea	53.12 ± 2.92	54.14 ± 3.36	0.082
Superior-hemi	53.43 ± 2.88	54.06 ± 3.56	0.292
Inferior-hemi	52.81 ± 3.25	54.21 ± 3.39	0.026
Temporal	53.24 ± 3.07	54.06 ± 3.73	0.199
Superior	53.80 ± 3.27	54.31 ± 3.94	0.452
Nasal	52.54 ± 2.96	53.45 ± 3.24	0.120
Inferior	52.88 ± 4.00	54.73 ± 3.72	0.012
Perifovea	50.81 ± 2.75	52.23 ± 2.02	0.002
Superior-hemi	50.82 ± 2.86	52.39 ± 2.08	0.001
Inferior-hemi	50.81 ± 2.81	52.06 ± 2.25	0.010
Temporal	47.98 ± 2.92	49.16 ± 2.36	0.019
Superior	50.55 ± 3.22	52.11 ± 2.42	0.004
Nasal	54.16 ± 2.86	55.71 ± 2.44	0.002
Inferior	50.56 ± 3.08	51.92 ± 2.36	0.010
Vessel density, DCP flow (%)			
Whole retina	54.87 ± 4.58	56.06 ± 4.54	0.166
Superior-hemi	55.40 ± 4.61	56.57 ± 4.72	0.182
Inferior-hemi	54.32 ± 4.76	55.53 ± 4.60	0.172
Fovea	38.62 ± 6.43	38.58 ± 7.91	0.975
Parafovea	57.88 ± 3.64	58.95 ± 3.74	0.124
Superior-hemi	58.37 ± 3.59	59.18 ± 3.96	0.250
Inferior-hemi	57.39 ± 3.89	58.71 ± 3.79	0.069
Temporal	58.78 ± 3.45	59.65 ± 3.96	0.208
Superior	57.70 ± 4.15	58.77 ± 4.22	0.173
Nasal	58.67 ± 3.85	59.26 ± 3.94	0.421
Inferior	56.38 ± 4.43	58.11 ± 4.26	0.036
Perifovea	56.39 ± 4.77	58.11 ± 4.26	0.214
Superior-hemi	56.99 ± 4.59	58.05 ± 4.84	0.228
Inferior-hemi	55.79 ± 5.18	56.98 ± 5.06	0.217
Temporal	57.70 ± 4.08	59.22 ± 3.68	0.040
Superior	56.54 ± 4.98	57.64 ± 5.60	0.270
Nasal	55.90 ± 5.36	56.66 ± 5.63	0.461
Inferior	55.41 ± 5.74	56.52 ± 5.89	0.311
RPC density, optic disk			
Whole	48.28 ± 2.41	50.14 ± 2.04	< 0.001
Inside disk	52.46 ± 3.88	53.58 ± 3.69	0.115
Peripapillary	49.22 ± 2.87	51.21 ± 2.50	< 0.001
Superior-hemi	49.10 ± 3.05	51.16 ± 2.51	< 0.001
Inferior-hemi	49.31 ± 3.01	51.25 ± 3.02	0.001

Abbreviations: *SCP*, superficial capillary plexus; *DCP*, deep capillary plexus; *RPC*, radial peripapillary capillary

*The values are presented as mean ± standard deviation

[a] Independent samples t test

Table 4 Correlation analyses between capillary density and other parameters in study groups

	VD(SCP)–whole retina		VD(SCP)–fovea		VD(SCP)–parafovea		VD(SCP)–perifovea		VD(DCP)–perifovea		VD(OD)–whole disk		VD(OD)–peripapillary	
Parameters	*r*	*p*	*r*	*p*	*r*	*p*	*r*	*p*	*r*	*p*	*r*	*p*	*r*	*p*
Hb	0.038	0.770	−0.026	0.842	0.043	0.741	0.031	0.810	0.284	0.025	0.031	0.810	−0.024	0.853
MCV	0.354	0.005	−0.449	*< 0.001*	0.318	0.012	0.381	0.002	0.257	0.043	0.498	< 0.001	0.515	< 0.001
Serum iron	−0.045	0.731	0.365	0.003	−0.110	0.396	−0.041	0.749	−0.205	0.111	−0.070	0.588	−0.074	0.568
TIBC	−0.060	0.644	−0.498	< 0.001	0.094	0.466	−0.052	0.688	0.161	0.212	−0.021	0.870	−0.016	0.899
Ferritin	0.317	0.012	0.049	0.706	0.253	0.047	0.300	0.018	0.076	0.559	0.162	0.208	0.103	0.424

Abbreviations: *Hb*, hemoglobin; *MCV*, mean corpuscular volume; *TIBC*, total iron-binding capacity; *VD*, vessel density; *SCP*, superficial capillary plexus; *DCP*, deep capillary plexus; *OD*, optic disk

Results

Demographic characteristics

The study involved 62 eyes of 62 participants. The study group included 32 IDA patients, while the control group consisted of 30 healthy volunteers. The study group comprised 20 (62.5%) females and 12 (37.5%) males, and the control group comprised 16 (53.4%) females and 14 (46.6%) males ($p = 0.363$). The mean age was 12.22 ± 4.48 years (range 5–18 years) in the study group and 12.37 ± 3.76 years (range 6–18 years) in the control group ($p = 0.843$). There was no statistically significant difference between age and gender in both groups ($p > 0.05$). There were statistically significant differences in Hb, MCV, serum iron, TIBC, and ferritin between the study and control groups ($p < 0.001$). The demographic characteristics of the study and the control groups are shown in Table 1.

OCT-A examinations

The mean values of the non-flow and FAZ assessment tool parameters in the study and control groups are shown in Table 2. There were no statistically significant differences between the groups for NFA, FAZ, PERIM, AI, and FD ($p > 0.05$). A statistically significant difference in SCP densities was found between the two groups in multiple quadrants ($p < 0.05$). Although a statistically significant difference in DCP densities was found between the two groups in several quadrants ($p < 0.05$), generally, no statistically significant difference was found ($p > 0.05$). In the analysis of the optic

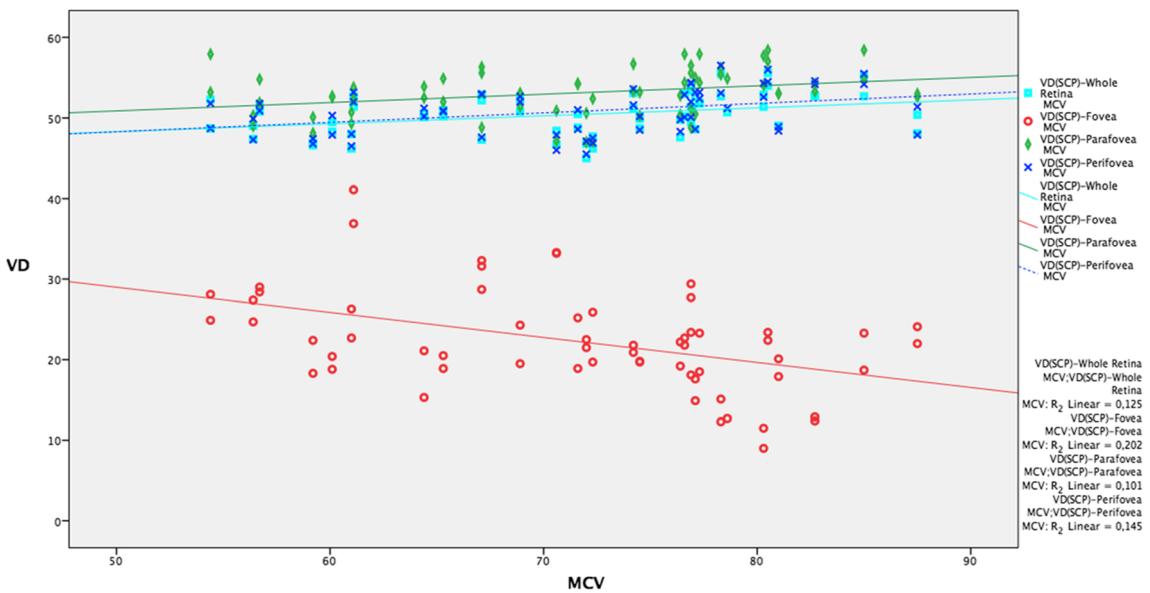

Fig. 4 Relationship between mean corpuscular volume (MCV) and vessel density (VD) of the superficial capillary plexus (SCP). Scatter plot showing positive correlations between MCV and VD (SCP) of the whole retina, perifovea, and parafovea. Scatter plot showing positive correlations between MCV and VD (SCP) of the fovea

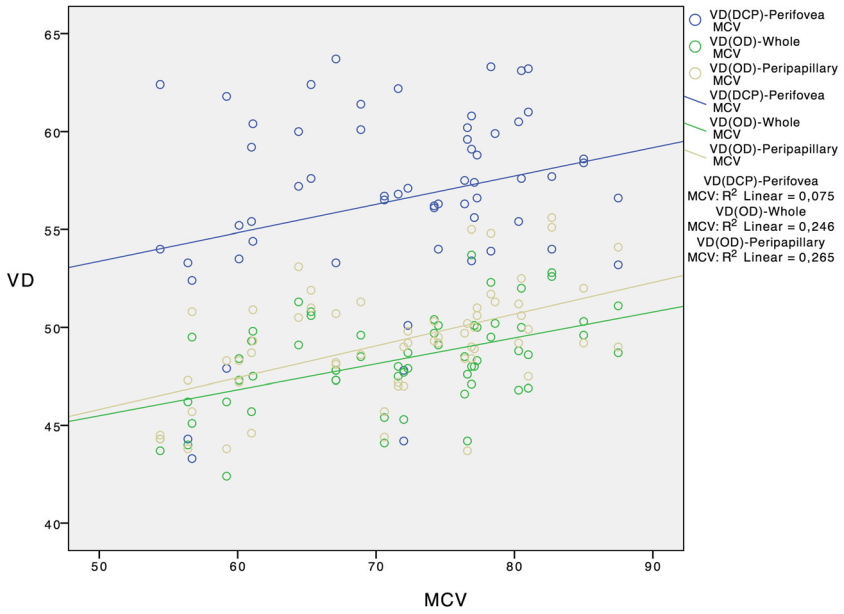

Fig. 5 Relationship between mean corpuscular volume (MCV) and vessel density (VD) of the deep capillary plexus (DCP) and optic disk (OD) area. Scatter plot showing positive correlations between MCV and VD (DCP) of the perifovea, and VD (OD) whole and peripapillary

disk base, a statistically significant difference was found in the other areas except from capillary density in the disk ($p < 0.05$). OCT-A device data of DCP and SCP densities in the different quadrants in the foveal, perifoveal, and parafoveal areas were summarized in Table 3.

In the study group, a correlation analysis of the hematological parameters including iron, TIBC, MCV, and ferritin levels and capillary densities showed a negative correlation between vascular densities and serum iron and TIBC, and a positive correlation with Hb, MCV, and ferritin levels. The correlations between hematologic parameters and capillary density are summarized in Table 4 and Figs. 4, 5, 6, 7, 8, and 9.

Discussion

In the current study, we evaluated capillary densities qualitatively in IDA children by the OCT-A device. Thus, we aimed to identify possible changes which could decrease visual level in the patients. To our knowledge, our study is the first to evaluate retinal microvascular changes in children with IDA by using OCT-A.

Central retinal vein occlusion, retinal hemorrhage, ischemic retinopathy, and papilledema are ocular manifestations reported in IDA patients [12, 13]. The exact pathophysiology of fundus lesions is unknown; however, it is considered that it might be associated with hypoxia [14]. Anemia causes chronic tissue hypoxia depending on its severity [15]. In our study,

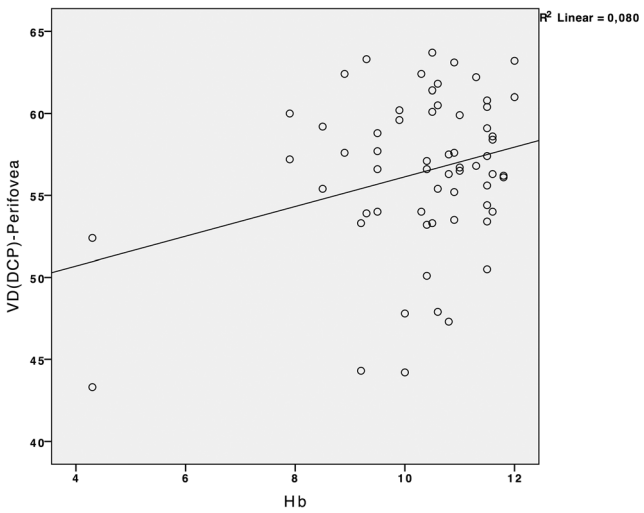

Fig. 6 Relationship between vessel density (VD) of the deep capillary plexus (DCP)–perifovea and hemoglobin (Hb). Scatter plot showing positive correlations between Hb and VD (DCP)–perifovea

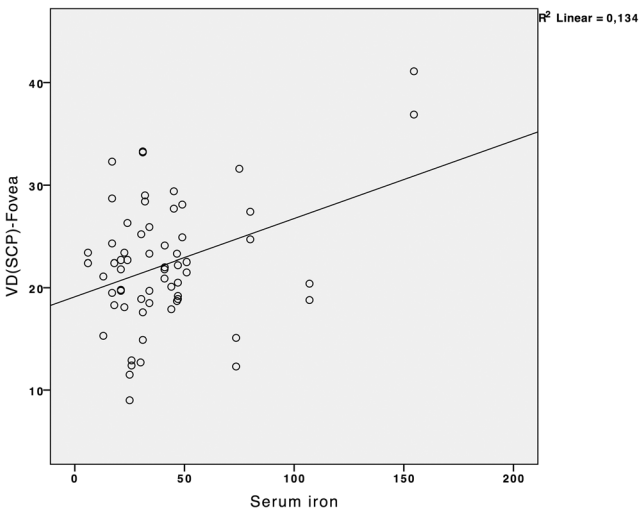

Fig. 7 Relationship between vessel density (VD) of superficial capillary plexus (SCP)–fovea and serum iron. Scatter plot showing positive correlations between serum iron and VD (SCP)–fovea

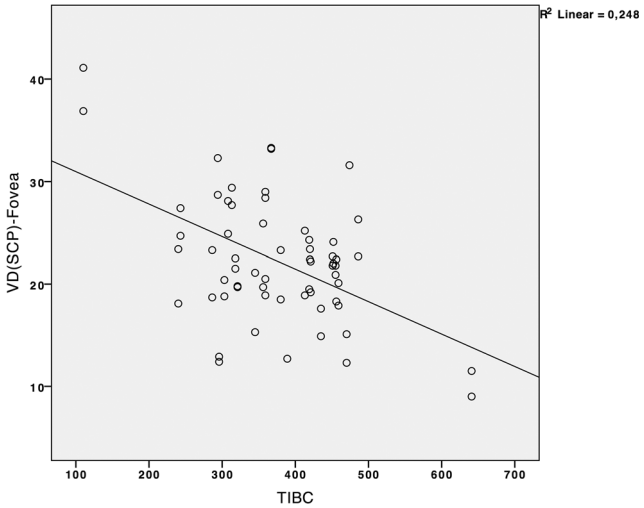

Fig. 8 Relationship between vessel density (VD) of the superficial capillary plexus (SCP)–fovea and total iron-binding capacity (TIBC). Scatter plot showing negative correlations between TIBC and VD (SCP)–fovea

we identified a positive correlation between decreased Hb and decreased SCP density in the perifoveal area. This is important to identify ischemia in the early period in IDA patients.

The photoreceptor cells persistently shed and resynthesize the outer layers. They contain disk membranes in the outer layer, and new membrane synthesis requires enzymes containing iron [16]. The choroid is located between the retina and the sclera, and contains many vascular beds, supplying nutrients and oxygen to the retinal tissues containing retinal pigment epithelium and photoreceptors. As a result, any structural or functional changes in the choroid blood flow cause a negative effect on the retina [17]. Şimsek et al. [14] showed that the choroidal thickness is decreased in children with ID. Aksoy et al. showed in their study that the retinal nerve fiber layer is thinned in children with ID [18]. Türkyılmaz et al. [19] reported a thinning in the average retinal nerve fiber layer and retinal nerve fiber layer superior and inferior quadrants in the patients with ID compared with the control group. Carraro et al. [13] reported that severe anemia plays an important role in the physiopathology of retinal anomalies. Foulds et al. [20] reported that prevalence of retinopathy increased in patients with Hb levels lower than 6 g/dL; however, Aisen et al. [21] reported that retinopathy may occur regardless of the severity or type of anemia. In our study, we found that capillary plexus density decreased by 4.5 × 4.5 mm in both the retinal 6 × 6 region and the optic disk region in children with IDA. It is noteworthy that the findings of decreased capillary plexus are in line with other studies in the literature. Besides, it is shown that capillary density decreased as serum iron levels decreased in the metabolically active foveal area. Likewise, capillary density decreased in the foveal area and showed a negative correlation as the capacity of binding iron increases.

It is known that iron has important functions in central nervous system metabolism, including nerve myelinization and neurotransmitter synthesis. Oligodendrocytes are very important for myelination, and ID impairs the normal function of these cells. Since iron is a cofactor in cholesterol and lipid biosynthesis, it affects myelin synthesis directly, while affecting indirectly as an oxidative metabolism component of oligodendrocytes [6]. Iron deficiency is also known to be associated with dopaminergic dysfunction. Dopamine is a well-known major neurotransmitter or modulator in the retina [19]. Lozoff et al. [22] have shown that infants with IDA had reduced spontaneous eye blinking rate by triggering dopaminergic dysfunction. In addition, malnutrition and deficiency of trace elements (including iron, zinc, and copper) may cause adverse changes on the optic nerves. SCP is located in the layer of ganglion cells. Ganglion cells decrease in neurodegenerative diseases including glaucoma. Iron deficiency

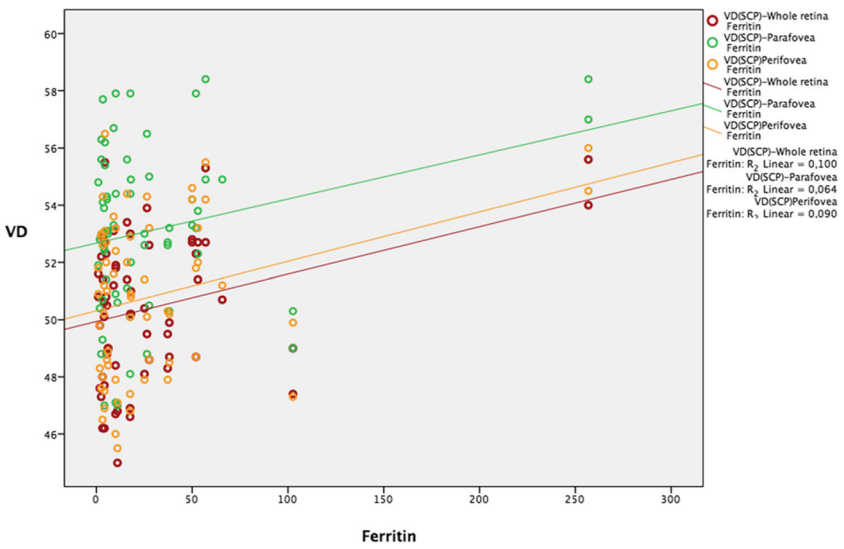

Fig. 9 Relationship between vessel density (VD) and ferritin of the superficial capillary plexus (SCP) area. Scatter plot showing positive correlations between ferritin and VD (SCP)–whole, parafovea, and perifoveal regions

is also known to have neurodegenerative effects [5, 16, 19, 23]. Therefore, the changes we detected may have been due to ganglion cell damage of iron deficiency.

Several blood abnormalities including ID may impair retinochoroidal circulation in the young patient group without atherosclerosis expectancy. It causes occlusion in the retinal veins and arteries [12]. The exact mechanism of this retinochoroidal effect in IDA patients is unknown; however, it is considered that ID affects the blood flow pattern in the vessels by increasing the viscosity of microcytic red blood cells and decreasing deformability, thus creating a hypercoagulable condition [14]. We can observe the movement of erythrocytes in the vessels by the OCT-A device, and learn about the retinal microvascular structure. In the studies performed by this device, several retinal microvascular pathologies including microaneurysm, capillary loss, increased capillary tortuosity, enlarged capillary loops, decreased capillary perfusion areas, irregularity of FAZ borders, and FAZ expansion have been identified [24, 25]. In our study, we also identified a decrease of capillary density that may be associated with capillary loss secondary to ID.

Optical coherence tomography angiography technology is an important development in ophthalmology to observe different retina capillary layers, and is an imaging method that can be used non-invasively without the need of fluorescein sodium contrast agent injection [26]. Previously, clinicians could observe vessels such as perifoveal superficial and deep capillary networks only by histological examination; however, OCT-A allows 3-dimensional images of their microarchitecture for the first time. However, OCT-A could not show the leakages and contains unknown artifacts especially in the deep plexus [27, 28]. Since the availability of OCT-A, there have been several studies that have reported the changes of retinal microvasculature in some childhood diseases [9–11].

The FAZ is the area of metabolically active photoreceptors responsible for central vision. FAZ area expansion has been detected in the course of several diseases, especially diabetes mellitus [29, 30]. It is reported that FAZ expansion is directly proportional with the severity of vision loss. But the literature showed that FAZ changes are not always present even though there are morphological changes in retinal capillaries [31]. Our study is also important because it showed that capillary density is used as a parameter to predict capillary loss in a specific area before the development of FAZ changes.

Strengths and limitations

The strengths of the study include the prospective nature of patients' recruitment and, to our knowledge, our study is the first to evaluate retinal microvascular changes in children with IDA using OCT-A. However, this study has several limitations. The number of patients was low due to poor patient cooperation in the pediatric group during OCT-A screening. Information on macular anatomy in children is very limited. Normal values were not reported in children undergoing OCT-A. Therefore, the literature that we can compare our study with is very limited. Finally, there is a need to investigate whether OCT-A would make a suitable screening technique for IDA in children.

In conclusion, it is important to identify the changes in retinal vascular structures by OCT-A in the early period to prevent possible ocular complications in children with IDA. Our study showed that these changes are correlated with the hematological parameters of ID. Wide-range studies are required in the future to use as criteria for the evaluation of decreased capillary density correlated with the severity of ID.

Acknowledgments We would like to thank the patients for taking part in this research.

Compliance with ethical standards

Conflict of interest The authors declare that they have no conflict of interest.

Ethical approval All procedures performed in studies involving human participants were in accordance with the ethical standards of the Institutional Review Board of University of Health Sciences Yuksek Ihtisas Training and Research Hospital and with the 1964 Helsinki declaration and its later amendments or comparable ethical standards.

Informed consent Informed consent was obtained from all individual participants included in the study.

References

1. McDonagh MS, Blazina I, Dana T, Cantor A, Bougatsos C (2015) Screening and routine supplementation for iron deficiency anemia: a systematic review. Pediatrics 135(4):723–733. https://doi.org/10.1542/peds.2014-3979
2. Domellof M, Thorsdottir I, Thorstensen K (2013) Health effects of different dietary iron intakes: a systematic literature review for the 5th Nordic Nutrition Recommendations. Food Nutr Res 57. https://doi.org/10.3402/fnr.v57i0.21667
3. Beard JL, Connor JR (2003) Iron status and neural functioning. Annu Rev Nutr 23:41–58. https://doi.org/10.1146/annurev.nutr.23.020102.075739
4. Yager JY, Hartfield DS (2002) Neurologic manifestations of iron deficiency in childhood. Pediatr Neurol 27(2):85–92
5. Cikmazkara I, Ugurlu SK (2016) Peripapillary retinal nerve fiber layer thickness in patients with iron deficiency anemia. Indian J Ophthalmol 64(3):201–205. https://doi.org/10.4103/0301-4738.181753
6. Akdogan E, Turkyilmaz K, Ayaz T, Tufekci D (2015) Peripapillary retinal nerve fibre layer thickness in women with iron deficiency anaemia. J Int Med Res 43(1):104–109. https://doi.org/10.1177/0300060514555562
7. Wylegala A, Teper S, Dobrowolski D, Wylegala E (2016) Optical coherence angiography: a review. Medicine 95(41):e4907. https://doi.org/10.1097/md.0000000000004907

8. de Carlo TE, Romano A, Waheed NK, Duker JS (2015) A review of optical coherence tomography angiography (OCTA). Int J Retin Vitr 1:5. https://doi.org/10.1186/s40942-015-0005-8
9. Roemer S, Bergin C, Kaeser PF, Ambresin A (2018) Assessment of macular vasculature of children with sickle cell disease compared to that of healthy controls using optical coherence tomography angiography. Retina. https://doi.org/10.1097/IAE.0000000000002321
10. Chen YC, Chen YT, Chen SN (2019) Foveal microvascular anomalies on optical coherence tomography angiography and the correlation with foveal thickness and visual acuity in retinopathy of prematurity. Graefes Arch Clin Exp Ophthalmol 257(1):23–30. https://doi.org/10.1007/s00417-018-4162-y
11. Niestrata-Ortiz M, Fichna P, Stankiewicz W, Stopa M (2019) Enlargement of the foveal avascular zone detected by optical coherence tomography angiography in diabetic children without diabetic retinopathy. Graefes Arch Clin Exp Ophthalmol 257(4):689–697. https://doi.org/10.1007/s00417-019-04264-8
12. Kacer B, Hattenbach LO, Horle S, Scharrer I, Kroll P, Koch F (2001) Central retinal vein occlusion and nonarteritic ischemic optic neuropathy in 2 patients with mild iron deficiency anemia. Ophthalmologica 215(2):128–131. https://doi.org/10.1159/000050843
13. Carraro MC, Rossetti L, Gerli GC (2001) Prevalence of retinopathy in patients with anemia or thrombocytopenia. Eur J Haematol 67(4):238–244
14. Simsek A, Tekin M, Bilen A, Karadag AS, Bucak IH, Turgut M (2016) Evaluation of choroidal thickness in children with iron deficiency anemia. Invest Ophthalmol Vis Sci 57(14):5940–5944. https://doi.org/10.1167/iovs.15-18713
15. Haase VH (2013) Regulation of erythropoiesis by hypoxia-inducible factors. Blood Rev 27(1):41–53. https://doi.org/10.1016/j.blre.2012.12.003
16. He X, Hahn P, Iacovelli J, Wong R, King C, Bhisitkul R, Massaro-Giordano M, Dunaief JL (2007) Iron homeostasis and toxicity in retinal degeneration. Prog Retin Eye Res 26(6):649–673. https://doi.org/10.1016/j.preteyeres.2007.07.004
17. Shao Z, Dorfman AL, Seshadri S, Djavari M, Kermorvant-Duchemin E, Sennlaub F, Blais M, Polosa A, Varma DR, Joyal JS, Lachapelle P, Hardy P, Sitaras N, Picard E, Mancini J, Sapieha P, Chemtob S (2011) Choroidal involution is a key component of oxygen-induced retinopathy. Invest Ophthalmol Vis Sci 52(9):6238–6248. https://doi.org/10.1167/iovs.10-6742
18. Aksoy A, Aslan L, Aslankurt M, Eser O, Garipardic M, Okumus S, Kaya G (2014) Retinal fiber layer thickness in children with thalessemia major and iron deficiency anemia. Semin Ophthalmol 29(1):22–26. https://doi.org/10.3109/08820538.2013.839811
19. Turkyilmaz K, Oner V, Ozkasap S, Sekeryapan B, Dereci S, Durmus M (2013) Peripapillary retinal nerve fiber layer thickness in children with iron deficiency anemia. Eur J Ophthalmol 23(2):217–222. https://doi.org/10.5301/ejo.5000206
20. Foulds WS (1963) The ocular manifestations of blood diseases. Trans Ophthalmol Soc UK 83:345–367
21. Aisen ML, Bacon BR, Goodman AM, Chester EM (1983) Retinal abnormalities associated with anemia. Arch Ophthalmol 101(7):1049–1052. https://doi.org/10.1001/archopht.1983.01040020051008
22. Lozoff B, Armony-Sivan R, Kaciroti N, Jing Y, Golub M, Jacobson SW (2010) Eye-blinking rates are slower in infants with iron-deficiency anemia than in nonanemic iron-deficient or iron-sufficient infants. J Nutr 140(5):1057–1061. https://doi.org/10.3945/jn.110.120964
23. Acar NO, Dadaci Z, Cetiner F, Yildiz M, Alptekin H, Borazan M (2016) Evaluation of the peripapillary retinal nerve fiber layer and ganglion cell-inner plexiform layer measurements in patients with iron deficiency anemia with optical coherence tomography. Cutan Ocul Toxicol 35(2):131–136. https://doi.org/10.3109/15569527.2015.1067228
24. Matsunaga DR, Yi JJ, De Koo LO, Ameri H, Puliafito CA, Kashani AH (2015) Optical coherence tomography angiography of diabetic retinopathy in human subjects. Ophthalmic Surg Lasers Imaging Retina 46(8):796–805. https://doi.org/10.3928/23258160-20150909-03
25. Hwang TS, Jia Y, Gao SS, Bailey ST, Lauer AK, Flaxel CJ, Wilson DJ, Huang D (2015) Optical coherence tomography angiography features of diabetic retinopathy. Retina 35(11):2371–2376. https://doi.org/10.1097/IAE.0000000000000716
26. Ting DSW, Tan GSW, Agrawal R, Yanagi Y, Sie NM, Wong CW, San Yeo IY, Lee SY, Cheung CMG, Wong TY (2017) Optical coherence tomographic angiography in type 2 diabetes and diabetic retinopathy. JAMA Ophthalmol 135(4):306–312. https://doi.org/10.1001/jamaophthalmol.2016.5877
27. Bradley PD, Sim DA, Keane PA, Cardoso J, Agrawal R, Tufail A, Egan CA (2016) The evaluation of diabetic macular ischemia using optical coherence tomography angiography. Invest Ophthalmol Vis Sci 57(2):626–631. https://doi.org/10.1167/iovs.15-18034
28. Hwang TS, Gao SS, Liu L, Lauer AK, Bailey ST, Flaxel CJ, Wilson DJ, Huang D, Jia Y (2016) Automated quantification of capillary nonperfusion using optical coherence tomography angiography in diabetic retinopathy. JAMA Ophthalmol 134(4):367–373. https://doi.org/10.1001/jamaophthalmol.2015.5658
29. Freiberg FJ, Pfau M, Wons J, Wirth MA, Becker MD, Michels S (2016) Optical coherence tomography angiography of the foveal avascular zone in diabetic retinopathy. Graefes Arch Clin Exp Ophthalmol 254(6):1051–1058. https://doi.org/10.1007/s00417-015-3148-2
30. Chang MY, Phasukkijwatana N, Garrity S, Pineles SL, Rahimi M, Sarraf D, Johnston M, Charles A, Arnold AC (2017) Foveal and peripapillary vascular decrement in migraine with aura demonstrated by optical coherence tomography angiography. Invest Ophthalmol Vis Sci 58(12):5477–5484. https://doi.org/10.1167/iovs.17-22477
31. Carnevali A, Sacconi R, Corbelli E, Tomasso L, Querques L, Zerbini G, Scorcia V, Bandello F, Querques G (2017) Optical coherence tomography angiography analysis of retinal vascular plexuses and choriocapillaris in patients with type 1 diabetes without diabetic retinopathy. Acta Diabetol 54(7):695–702. https://doi.org/10.1007/s00592-017-0996-8